A Rationally Designed Connector for Assembly of Protein-Functionalized DNA Nanostructures

Katja J. Koßmann, Cornelia Ziegler, Alessandro Angelin, Rebecca Meyer, Marc Skoupi, Kersten S. Rabe, and Christof M. Niemeyer*[a]

We report on the rational engineering of the binding interface of the self-ligating HaloTag protein to generate an optimized linker for DNA nanostructures. Five amino acids positioned around the active-site entry channel for the chlorohexyl ligand (CH) of the HaloTag protein were exchanged for positively charged lysine amino acids to produce the HOB (halo-based oligonucleotide binder) protein. HOB was genetically fused with the enzyme cytochrome P450 BM3, as well as with BMR, the separated reductase domain of BM3. The resulting HOB-fusion proteins revealed significantly improved rates in ligation with CH-modified oligonucleotides and DNA origami nanostructures. These results suggest that the efficient self-assembly of protein-decorated DNA structures can be greatly improved by fine-tuning of the electrostatic interactions between proteins and the negatively charged nucleic acid nanostructures.

The invention of the so-called "scaffolded DNA origami" technique[1] has opened the door to an almost unlimited variety of finite DNA nanostructures.[2,3] Such objects possess addressable surfaces that can be decorated with functional units with a single "pixel" resolution of about 6 nm.[4] Therefore, DNA origami nanostructures (DONs) are extensively exploited as molecular pegboards for the precise positioning of proteins or nanoparticles.[4–9] The use of proteins is particularly promising because these biomacromolecules have evolutionarily optimized functionalities, such as the capability for specific molecular recognition and catalytic conversion of ligands and substrates.[10] Arrangements of synthetic multienzyme cascades on DNA nanostructures, for example, are currently being exploited as spatially interactive biomolecular networks.[11]

This research is hampered by the fact that most enzymes are difficult to immobilize, due to their delicate tertiary structures, which can easily be harmed by coupling and purification methods, going along with a decrease in catalytic activity. Owing to these restrictions, the majority of reports on origami-based multi-enzyme assemblies have used stable, commercially available glucose oxidase (GOx)/horseradish peroxidase (HRP)[12–16] or glucose-6-phosphate dehydrogenase (G6PDH)/malic dehydrogenase (MDH)[17] as model cascades. Only a few reports so far have involved sensitive recombinant proteins, such as oxidoreductases[18,19] or cytochrome P450 BM3 porphyrin/reductase domains,[19,20] produced by heterologous expression. Enzymes' instabilities also limit the possibilities for purification of DNA·enzyme constructs. Hence, there is a great demand for specific and efficient coupling reactions to install arbitrary proteins of interest (POIs) on DNA nanostructures.

To facilitate site-selective conjugation of proteins with DNA origami scaffolds under mild conditions, we have previously developed a methodology based on the genetic fusion of the POIs with self-labeling protein tags:[19–22] that is, the "SnapTag",[23] and the "HaloTag®".[24] In this process, benzylguanine (BG) or chlorohexane (CH) groups are incorporated as suicide ligands into DNA nanostructures to facilitate orthogonal binding of Snap- and Halo-tagged POIs, respectively. Although these systems reveal excellent specificity and are conveniently applicable, even on a preparative scale,[19,20] there is still room for improvement of coupling efficacies. Specifically, for binding to DONs, typical coupling rates of Snap- and Halo-tagged POIs were in the range of 40–60% even though large excesses of about 100–1000 molar equivalents of POI per suicide ligand were used.[19,21]

In the course of these studies we observed that the charges of the proteins greatly influence the coupling efficacy. Proteins with lower isoelectric point (pIs) bound less efficiently than those with higher pIs, thus suggesting that protein binding is significantly influenced by electrostatic interactions between the negatively charged DONs and the POIs.[19,21,25] We therefore reasoned that the coupling might be improved by rational design of a positively charged interface between the POI's fusion tag and the negatively charged DNA nanostructure. As a proof of concept, here we report the development of a HaloTag variant genetically engineered to contain five positively charged lysine residues at its binding interface (Figure 1). This new halo-based oligonucleotide binder (HOB) protein can be readily fused with arbitrary POIs. The resulting fusion proteins reveal significantly improved rates in coupling with CH-modified oligonucleotides, thereby enabling their fast and efficient immobilization on DNA origami nanostructures.

To improve the commercially available HaloTag protein, we initially analyzed the reported X-ray crystal structure (PDB ID: 4KAF) to identify amino acids for exchange for positively charged residues. It is shown in Figure 1 that the entry channel

[a] *K. J. Koßmann, C. Ziegler, A. Angelin, Dr. R. Meyer, M. Skoupi, Dr. K. S. Rabe, Prof. Dr. C. M. Niemeyer*
Karlsruhe Institute of Technology (KIT)
Institute for Biological Interfaces (IBG 1)
Hermann von Helmholtz Platz 1
76344 Eggenstein Leopoldshafen (Germany)
E mail: niemeyer@kit.edu

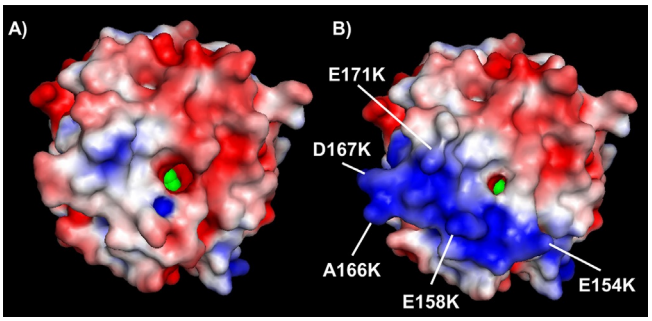

Figure 1. Electrostatic potential of A) the HaloTag protein, and B) the HOB protein around the active site entry channel, indicated by the colored green substrate. The HOB protein displays an increased positive charge (blue) around the channel entrance due to the indicated X→K amino acid mutations. The illustrated structures were generated with SWISS MODEL[26,27] and the repairPDB function from FoldX[28] and are based on the PDB ID: 4KAF; the substrate was superimposed from PDB ID: 4C6H. The electrostatic potential maps were calculated by use of the PDB ID: 2PQR[29] and APBS web servers[30] and visualized by use of the PyMOL molecular graphics system (version 1.8, Schrödinger, LLC). Numbering is analogous to that of the 4KAF structure.

leading up to the active site is dominated by a negative electrostatic potential (indicated by red) and contains several glutamic acid residues. We strove to create a patch of positively charged lysine residues in order to promote electrostatic attraction and a preferred binding orientation of the CH group tethered to the negatively charged nucleic acid. The chosen mutations were incorporated into the DNA sequence of the commercially available HaloTag as provided by the manufacturer (Promega).

The resulting DNA string for the new HOB protein was synthesized and recloned into the vector pDESTn9-BM3, previously developed for HaloTag-fusions of the enzyme cytochrome P450 BM3, as well as the separated reductase domain of BM3, termed BMR.[19,20] Three vectors were generated for heterologous expression of the fusion proteins containing the HOB portion at the N or the C terminus [HOB-BMR and BMR-HOB, respectively (molecular weights of ≈100 kDa), as well as BM3-HOB (MW≈158 kDa)]. The fusion proteins were expressed in *Escherichia coli* and purified to homogeneity (Figure S1 in the Supporting Information). Expression yields of 1.3, 1.3, 1.9, and 2.1 mg L^{-1} cell culture were obtained for BMR-HaloTag, HOB-BMR, BMR-HOB, and BM3-HOB, respectively. Furthermore, enzyme activity measurements indicated nearly identical catalytic activities of the HOB-fusion proteins, in relation to the HaloTag fusion enzymes (Figure S2). Interestingly, and for as yet unknown reasons, all BMR fusions revealed significantly higher activities than the untagged wild-type enzyme.

To investigate the coupling of CH-modified oligonucleotides with HOB fusion proteins, the 23-mer oligonucleotides tAm-F1 with terminal 5′ and iAm-F1 with internal (position 12) amino-modified thymine bases (amino-modifier-C6-dT, Sigma) were used for the attachment of the CH ligand. The internal modification served as a simplified model for a DON. The detailed oligonucleotide sequences and coupling procedures are given in the Supporting Information. Both oligonucleotides were coupled with the amine-reactive *N*-hydroxysuccinimide (NHS)-activated CH ligand to generate tCH-F1 and iCH-F1 oligomers, which were typically obtained in near quantitative yields, similarly to what has previously been described (Figure S3). Similar results were also obtained for amino-modified DON staple strands (Figure S4).[21] It should be noted, however, that modification efficacy depended on the quality of the particular amino-modified oligonucleotide batch. For instance, we observed that oligomers carrying the amino group at their 3′-ends showed significantly lower modification yields (≈75%) than 5′-modified oligomers (≈85%). Although the obtained modification efficacies were perfectly acceptable for this study, we note that routine quality control and, if necessary, subsequent purification of the CH-modified oligomers—by HPLC, for example (Figure S5)—is recommended when optimal yields are crucial for the anticipated application of DNA nanostructures decorated with Halo-tagged proteins.

To evaluate the influence of the mutated amino acids, we then investigated the coupling of tCH-F1 and iCH-F1 oligomers with HOB-BMR and BMR-HOB, along with the fusion protein BMR-Halo, containing the conventional HaloTag used in our previous studies.[19–22] To this end, the proteins (1.0 μM) were mixed with 1.3 molar equivalents of the oligomers tCH-F1 or iCH-F1 (1.3 μM), and the coupling was followed by gel electrophoresis, either with a denaturing SDS-PAGE to visualize the proteins (Figure 2) or with non-denaturing gels with nucleic acid staining (Figure S6). Time course experiments indicated significantly improved reaction rates of HOB-tagged BMR relative to the conventional BMR-HaloTag fusion. Owing to the low concentration and almost equimolar reactant ratio, BMR-Halo showed almost no reactivity under these conditions (Figure 2A). For comparison, complete conversion was observed for the BMR-HaloTag in earlier studies in which ≈200 molar equivalents of the protein were used.[19–22] Importantly, the coupling of the internally positioned CH ligand (oligomer iCH-F1) was significantly slower than that of the terminally modified oligomer tCH-F1 (blue and red points in Figure 2A). We assume that the different reaction rates of the two oligomers are due to differences in the electrostatic shielding and/or steric hindrance of the CH ligand. Notably, no such differences between iCH-F1 and tCH-F1 were observed upon coupling with the HOB fusions, in which reactions were completed in about 30 or <15 min for the BMR-HOB and HOB-BMR fusions, respectively. Kinetic analyses (Figure S6) revealed relative increases in velocity of approximately 1:5:20 for BMR-HaloTag, BMR-HOB, and HOB-BMR, respectively, and second-order rate constants significantly lower than the value previously determined for the coupling of GST-HaloTag with the small-molecule ligand TMR.[31] We assume that this difference is due to the much smaller size of the TMR ligand along with the lack of electrostatic repulsion. The relative kinetic data for BMR-HaloTag and the HOB proteins are in agreement with the changes in the isoelectric point (pI) values (HaloTag = 4.6, HOB = 5.4, Figure S6). However, these calculated global pI values represent the entire protein tag and do not take into account the local accumulation of positive charges engineered into the microenvironment around the entry channel of our HOB protein. The faster reaction rate for the N-terminal fusion HOB-BMR

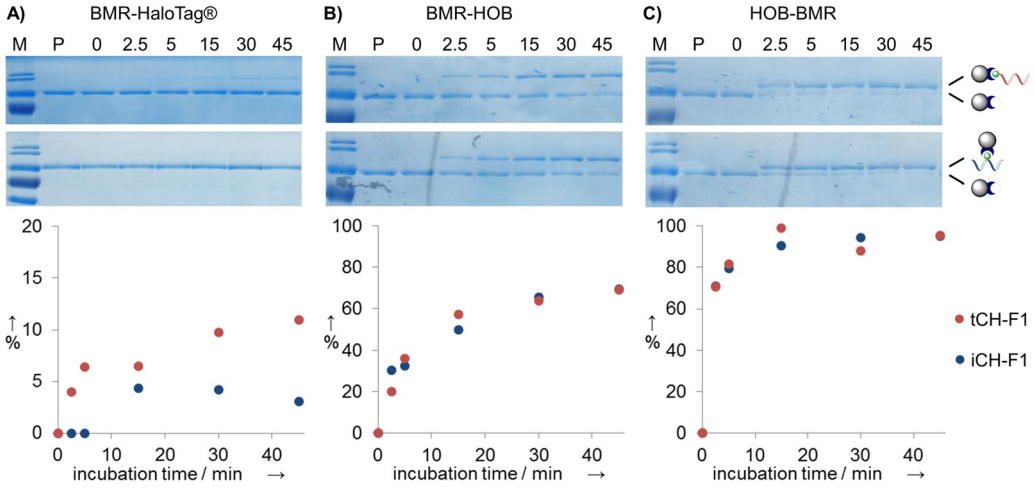

Figure 2. Binding of A) BMR HaloTag, B) BMR HOB, and C) HOB BMR with 22 mer oligonucleotides tCH F1 (red) or iCH F1 (blue), bearing the CH ligand (green) at the terminal 5′ or an internal thymine base position, respectively. The reactions were carried out with 1.0 μM protein and 1.3 μM oligonucleotide concentrations for variable times, indicated on top of the gels (12% SDS PAGE; M stands for Thermo Scientific PageRuler prestained protein ladder, and P stands for protein only). The formation of protein·DNA conjugates was quantified by densitometric analysis, and percentage of coupling was plotted against the reaction time. Note the different scale of the *y* axis in A).

might be due to better accessibility of the CH ligand entry channel (Figure S7). Despite its lower reactivity, we chose the C-terminal fusion BMR-HOB for further experiments, due to its higher purity and to enable direct side-by-side comparison with BMR-HaloTag.

On the basis of the results obtained from oligonucleotide coupling, we tested the binding of BMR-HOB to a rectangular ≈54 × ≈91 nm^2 DNA origami nanostructure, which was assembled from the single-stranded 5438 nt template 109Z5.[32] It contained six binding sites located at distinguishable positions (B1–B6) on the rectangular plate (Figure 3; for a schematic illustration, see Figure S11 A). The DON (50 nM) was mixed with the proteins, with use of either one or three molar equivalents with respect to the six CH binding sites, and samples were taken after 15, 60, and 120 min for AFM analysis and statistical evaluation of the images (Figure 3). As expected, surface occupancies increased over time. Prolonged incubation times (> 2 h) were avoided, to prevent detrimental effects on the enzymatic activity.[19]

Coupling of 1 equiv of either BMR-HOB or the conventional BMR-HaloTag led to average surface occupancies of 31% or only 5%, respectively (Figure 3 A, B), thus clearly indicating the superior binding properties of the engineered HOB. Furthermore, binding of 3 equiv of BMR-HOB led to a surface occupancy of almost 80% (Figure 3 C). This result is outstanding because 80 molar equivalents of BMR-Halo were required in previous work to attain surface occupancies of only ≈26%.[19] It is important to note that the modification of CH-tagged DONs with only 3 equiv of proteins (Figure 3 C) enables the direct AFM imaging of crude samples without the necessity of extensive purification by ultrafiltration[21] or free-flow electrophoresis (see also Figure S8).[19] As a potential means to minimize adverse effects on the enzymatic activity, we also determined how a lower incubation temperature would influence the coupling efficacy. Specifically, when the coupling of the DON with 3 equiv BMR-HOB was carried out on an ice bath, we observed about half of the surface occupancy that was obtained at room temperature (40 vs. 80%, respectively, Figure S9).

Additional experiments carried out with the large HOB-tagged BM3 holoenzyme revealed surface occupancies of 34% (Figure 3 D) or 70% (Figure S10) when 1 or 3 molar equivalents, respectively, of the protein were allowed to bind on the DON. These results confirm the data obtained for binding of the smaller BMR-HOB and suggest that the immobilization of these fusion proteins is indeed primarily dominated by electrostatic interactions rather than by steric effects. Interestingly, we also found that coupling efficiency could not be improved by installment of two CH ligands in close proximity at directly adjoining positions of the origami (Figure S11). We expected that the increased local concentration of two adjacent ligands would increase coupling rates and compensate for missing CH groups due to incomplete chemical conversion (see above). However, neither HOB- nor HaloTag-tagged protein binding was significantly affected, thus suggesting that the additional synthetic effort necessary for introducing pairs of ligands is not paying off in terms of high protein binding capability of the DON.

In conclusion, here we have demonstrated the rational engineering of the binding interface of a self-ligating protein to generate an optimized linker for DNA nanostructures. Positively charged amino acids were incorporated around the active-site entry channel of the chlorohexyl ligand (CH) of the HaloTag protein to produce the HOB protein, which can be readily fused with arbitrary proteins of interest. The resulting HOB-fusion proteins revealed significantly improved rates in the ligation with CH-modified oligonucleotides and DNA origami nanostructures. Notably, the simplicity and general applicability of our approach has advantages over site-specific methods to improve protein loading of DONs, such as the fusion of Snap-tagged POIs with a zinc finger motif.[33] On the basis of our ini-

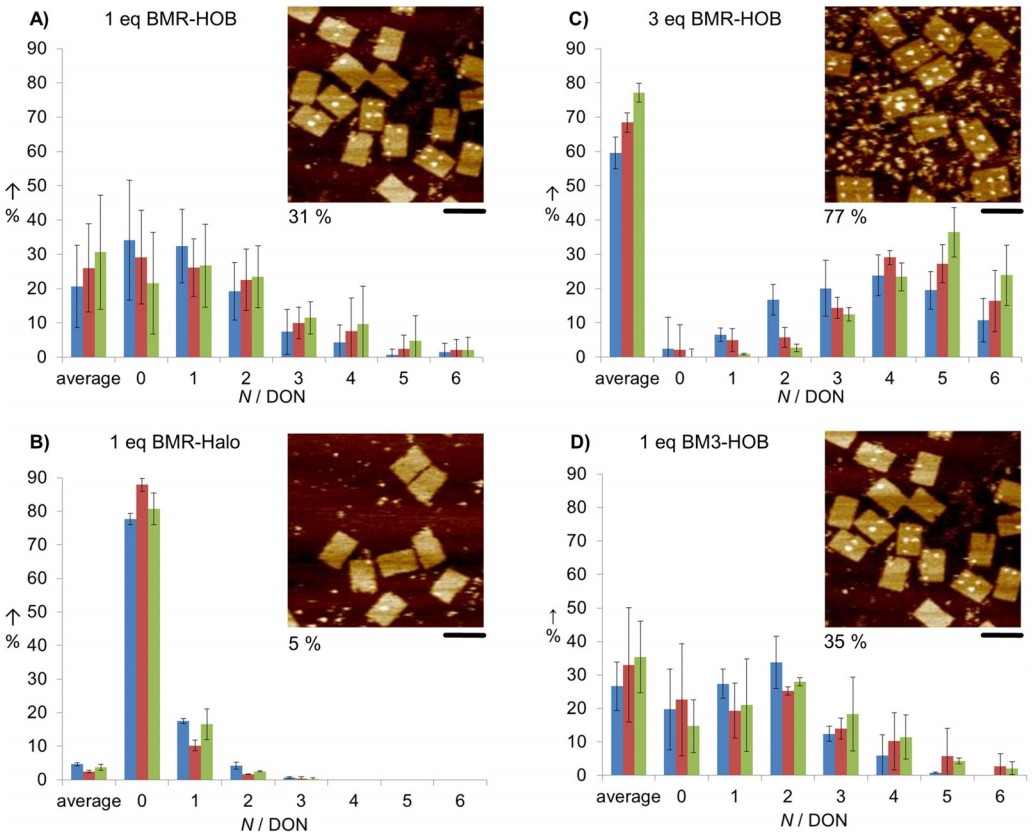

Figure 3. Decoration of DNA origami nanostructures. The bar diagrams show the average surface occupancies and the distributions of all structures with $N = 0$, 1, 2, 3, 4, 5 and 6 protein molecules per well formed DON, determined by AFM analysis after incubation for 15 min (blue), 60 min (red), or 120 min (green). Typically >500 DONs were counted for each experiment and time point. The insets show representative AFM images after 120 min reaction time; scale bars: 100 nm. Average surface occupancies (% of available CH groups covered with proteins) are indicated below.

tial results, we believe that engineering of electrostatic interactions is highly promising for further advancement of the generation and exploitation of protein-decorated DNA origami nanostructures in, for instance, the area of synthetic multienzyme cascades and other spatially interactive biomolecular networks[11] or as functional interfaces for living cells.[34]

Acknowledgements

This work was supported by the Deutsche Forschungsgemeinschaft through grant Ni399/10 and by the Helmholtz programme BioInterfaces in Technology and Medicine. We thank Anke Dech, Elisabeth Hirth, Alessa Schilling, and Jens Bauer for experimental help.

Keywords: bioconjugates · DNA nanostructures · enzymes · self-assembly

[1] P. W. Rothemund, *Nature* **2006**, *440*, 297 302.
[2] J. Nangreave, D. Han, Y. Liu, H. Yan, *Curr. Opin. Chem. Biol.* **2010**, *14*, 608 615.
[3] W. M. Shih, C. Lin, *Curr. Opin. Struct. Biol.* **2010**, *20*, 276 282.
[4] B. Saccà, C. M. Niemeyer, *Angew. Chem. Int. Ed.* **2012**, *51*, 58 66; *Angew. Chem.* **2012**, *124*, 60 69.
[5] A. M. Hung, H. Noh, J. N. Cha, *Nanoscale* **2010**, *2*, 2530 2537.
[6] T. Tørring, N. V. Voigt, J. Nangreave, H. Yan, K. V. Gothelf, *Chem. Soc. Rev.* **2011**, *40*, 5636 5646.
[7] F. C. Simmel, *Curr. Opin. Biotechnol.* **2012**, *23*, 516 521.
[8] A. Rajendran, M. Endo, H. Sugiyama, *Angew. Chem. Int. Ed.* **2012**, *51*, 874 890; *Angew. Chem.* **2012**, *124*, 898 915.
[9] Q. Liu, C. Song, Z. G. Wang, N. Li, B. Ding, *Methods* **2014**, *67*, 205 214.
[10] C. M. Niemeyer, *Angew. Chem. Int. Ed.* **2010**, *49*, 1200 1216; *Angew. Chem.* **2010**, *122*, 1220 1238.
[11] J. Fu, M. Liu, Y. Liu, H. Yan, *Acc. Chem. Res.* **2012**, *45*, 1215 1226.
[12] J. Müller, C. M. Niemeyer, *Biochem. Biophys. Res. Commun.* **2008**, *377*, 62 67.
[13] O. I. Wilner, S. Shimron, Y. Weizmann, Z. G. Wang, I. Willner, *Nano Lett.* **2009**, *9*, 2040 2043.
[14] O. I. Wilner, Y. Weizmann, R. Gill, O. Lioubashevski, R. Freeman, I. Willner, *Nat. Nanotechnol.* **2009**, *4*, 249 254.
[15] J. Fu, M. Liu, Y. Liu, N. W. Woodbury, H. Yan, *J. Am. Chem. Soc.* **2012**, *134*, 5516 5519.
[16] Y. Fu, D. Zeng, J. Chao, Y. Jin, Z. Zhang, H. Liu, D. Li, H. Ma, Q. Huang, K. V. Gothelf, C. Fan, *J. Am. Chem. Soc.* **2013**, *135*, 696 702.
[17] J. Fu, Y. R. Yang, A. Johnson Buck, M. Liu, Y. Liu, N. G. Walter, N. W. Woodbury, H. Yan, *Nat. Nanotechnol.* **2014**, *9*, 531 536.
[18] C. M. Niemeyer, J. Koehler, C. Wuerdemann, *ChemBioChem* **2002**, *3*, 242 245.
[19] C. Timm, C. M. Niemeyer, *Angew. Chem. Int. Ed.* **2015**, *54*, 6745 6750; *Angew. Chem.* **2015**, *127*, 6849 6854.
[20] M. Erkelenz, C. H. Kuo, C. M. Niemeyer, *J. Am. Chem. Soc.* **2011**, *133*, 16111 16118.
[21] B. Saccà, R. Meyer, M. Erkelenz, K. Kiko, A. Arndt, H. Schroeder, K. S. Rabe, C. M. Niemeyer, *Angew. Chem. Int. Ed.* **2010**, *49*, 9378 9383; *Angew. Chem.* **2010**, *122*, 9568 9573.
[22] R. Meyer, C. M. Niemeyer, *Small* **2011**, *7*, 3211 3218.

[23] A. Keppler, S. Gendreizig, T. Gronemeyer, H. Pick, H. Vogel, K. Johnsson, *Nat. Biotechnol.* **2002**, *21*, 86 89.
[24] G. V. Los, K. Wood, *Methods Mol. Biol.* **2007**, *356*, 195 208.
[25] M. Erkelenz, C. Junk, C. M. Niemeyer, unpublished results.
[26] K. Arnold, L. Bordoli, J. Kopp, T. Schwede, *Bioinformatics* **2006**, *22*, 195 201.
[27] L. Bordoli, F. Kiefer, K. Arnold, P. Benkert, J. Battey, T. Schwede, *Nat. Protoc.* **2008**, *4*, 1 13.
[28] J. Schymkowitz, J. Borg, F. Stricher, R. Nys, F. Rousseau, L. Serrano, *Nucle ic Acids Res.* **2005**, *33*, W382 W388.
[29] T. J. Dolinsky, P. Czodrowski, H. Li, J. E. Nielsen, J. H. Jensen, G. Klebe, N. A. Baker, *Nucleic Acids Res.* **2007**, *35*, W522 W525.
[30] N. A. Baker, D. Sept, S. Joseph, M. J. Holst, J. A. McCammon, *Proc. Natl. Acad. Sci. USA* **2001**, *98*, 10037 10041.
[31] G. V. Los, L. P. Encell, M. G. McDougall, D. D. Hartzell, N. Karassina, C. Zimprich, M. G. Wood, R. Learish, R. F. Ohana, M. Urh, D. Simpson, J. Mendez, K. Zimmerman, P. Otto, G. Vidugiris, J. Zhu, A. Darzins, D. H. Klaubert, R. F. Bulleit, K. V. Wood, *ACS Chem. Biol.* **2008**, *3*, 373 382.
[32] M. Erkelenz, D. M. Bauer, R. Meyer, C. Gatsogiannis, S. Raunser, B. Sacca, C. M. Niemeyer, *Small* **2014**, *10*, 73 77.
[33] E. Nakata, H. Dinh, T. A. Ngo, M. Saimura, T. Morii, *Chem. Commun.* **2015**, *51*, 1016 1019.
[34] A. Angelin, S. Weigel, R. Garrecht, R. Meyer, J. Bauer, R. K. Kumar, M. Hirtz, C. M. Niemeyer, *Angew. Chem. Int. Ed.* **2015**, *54*, 15813 15817; Angew. Chem. **2015**, 127, 16039 16043.